Stimulated Detonation of a High-Energy Heterogeneous Plasma Formation Created by a Capillary Erosive Plasma Generator and a Magneto-Plasma Compressor

Article *in* Russian Journal of Physical Chemistry B · December 2024

DOI: 10.1134/S1990793124701136

3 authors:

Anatoly Klimov

Russian Academy of Sciences

Vadim Brovkin

Объединённый Институт Высоких Температур РАН

Anatoly Pashchina

Joint Institute for High Temperatures, Russian Academy of Sciences

ISSN 1990-7931, Russian Journal of Physical Chemistry B, 2024, Vol. 18, No. 5, pp. 1415–1421. © Pleiades Publishing, Ltd., 2024.

CHEMICAL PHYSICS OF ATMOSPHERIC PHENOMENA

Stimulated Detonation of a High-Energy Heterogeneous Plasma Formation Created by a Capillary Erosive Plasma Generator and a Magneto-Plasma Compressor

A. I. Klimov[a, *], **V. G. Brovkin**[a], **and A. S. Pashchina**[a]

[a] *Joint Institute for High Temperatures, Russian Academy of Sciences, Moscow, Russia*

**e-mail: klimov.anatoly@gmail.com*

Received April 12, 2024; revised May 13, 2024; accepted May 20, 2024

Abstract—Studying the physical properties of long-lived plasma formations can help us understand the nature of electrophysical phenomena in thunder clouds, the lower ionosphere, tornadoes, volcanic activity, and the associated appearance of natural plasmoids (such as ball lightning, sprites, jets, etc.). The stimulated detonation of long-lived energy-consuming plasmoids (LEPs) obtained in a laboratory using a combined type of plasma generator consisting of an erosive plasma generator and a magnetoplasma compressor (MPC) is studied in this paper. It is found that a necessary condition for detonation is the excess of certain threshold values of pressure and temperature. The existence of a directed explosion mode is established, which is realized only at the optimal delay times (of the order of t_d ~ 2000 μs) between the beginning of a pulsed erosion discharge and the discharge of an MPC. The parameters of shock waves (SWs), as well as the optical and X-ray spectra of LEPs in the stimulated detonation mode are measured.

Keywords: plasma, magnetoplasma compressor, erosive discharge, detonation, shock wave

DOI: 10.1134/S1990793124701136

1. INTRODUCTION

Magnetoplasma compressors (MPCs) are widely used in research on plasma physics and plasma aerodynamics [1, 2]. In this device, the geometry of the electrodes and the parameters of the electrical discharge make it possible to obtain a local zone of plasma energy cumulation, called the *plasma focus* [3], with extremely high plasma parameters. Currently, such devices are used to produce low-energy neutron beams in research in plasma physics, flaw detection, customs, and other areas [4–7].

In [2], it was reported that a new combined plasma generator was first developed and tested, consisting of an MPC [1–3] and an erosive plasmatron (EP) based on a pulsed discharge in a capillary with an evaporating wall [8–11]. At the same time, instead of the traditional metal anode in the MPC, it was proposed to use an erosive plasma jet created by an EP [2, 8]. This combination (MPC-EP) made it possible to expand the operating pressure range of stable operation of the MPC up to atmospheric pressure and above it. At the first stage, the EP creates a long-lived energy-consuming plasmoid (LEP), which includes a heterophase consisting of metal and carbon nanosized clusters, as well as hydrogen atoms and ions. At the second stage, the MPC discharge is ignited, providing magnetic compression of the LEP and initiation of detonation processes in it. In [2], it was discovered that, under certain parameters of the plasma and electric discharge, stimulated detonation can occur inside the LEP. Note that this work has been widely read by physicists. According to the research portal Research Gate, it was read by more than 200 scientists in the past year alone.

This paper is a continuation of the research begun earlier [2, 8–13] and further studies the process of stimulated detonation of LEP depending on the time delay t_d between the moments of turning on the EP and MPC, as well as the search for the optimal mode of such detonation.

2. EXPERIMENTAL SETUP

The electrical circuit and general view of the combined MPC-EP discharger are shown in Fig. 1. In this installation, at the first stage, using an EP (*1*–*4*) an erosive plasma jet (*8*) is formed. At the same time, it acts as a plasma anode of the MPC, which is triggered at the second stage of the discharge with a certain delay t_d relative to the moment of the EP is turned on. The cathodes of the MPC are six copper rods (*7*), located on a circle of radius 16 mm and mounted on a cathode flange (*6*). The erosive plasma jet formed by

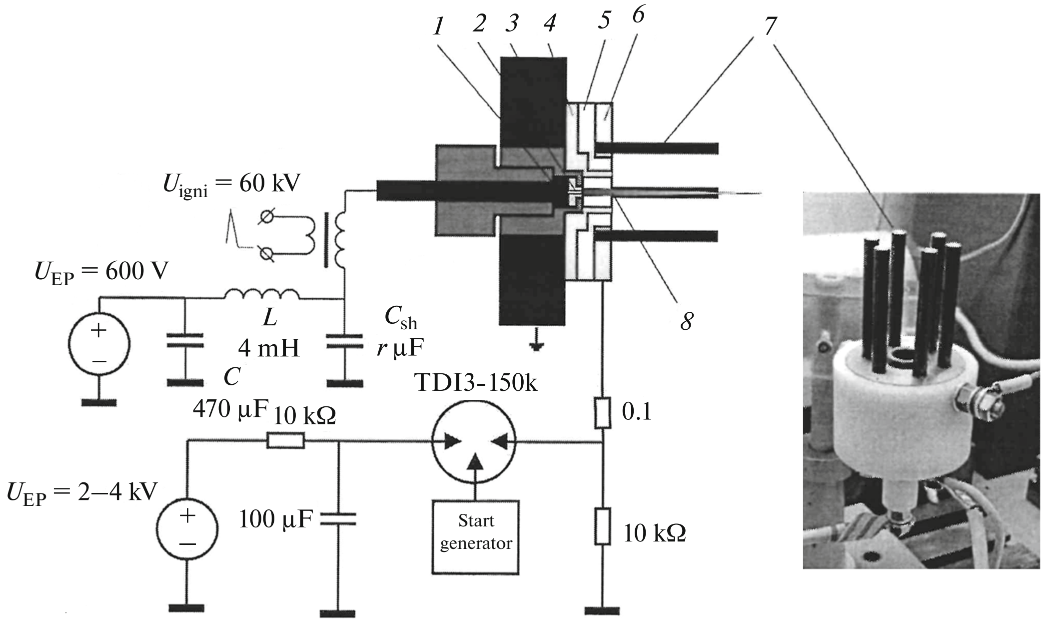

Fig. 1. Electrical diagram and general view of the MPC-EP combined discharger: (*1*) internal electrode (anode) of the EP; (*2*) capillary discharge channel of EP; (*3*) discharger housing; (*4*) EP cathode/MPC anode; (*5*) insulator; (*6*) cathode flange MPC; (*7*) MPC cathode rods; (*8*) heterogeneous plasma jet (LEP).

an EP is essentially an LEP with the given chemical composition. The typical values of the electron concentration and temperature in an LEP, respectively, are $n_e \approx 2 \times 10^{17}$ cm^{-3} and $T_e \approx 2$–3 eV [8, 10]. The plasma-chemical composition of the LEP depends on the eroding working material used in the discharge gap of the EP (*2*) and the material of eroding electrodes (*1*, *4*). Polymethyl methacrylate (PMMA), from which the EP capillary was made, was used as the tested working materials (*2* in Fig. 1), as well as titanium hydride (TiH_x) and nickel hydride (NiH_x), which in the form of powder or prepressed washers could be placed directly behind the outlet of the EP capillary. Nickel was used as the material for the internal electrode of the EP (anode, *1* in Fig. 1). The external electrode (cathode) of the EP (it is also the anode of the MPC, *4* in Fig. 1) and the MPC cathodes (*7*) were made of copper.

The second stage of the combined discharge includes compression and heating of the LEP plasma using the MPC discharge initiated with a certain time delay (t_d ~ 0.1–3 ms) relative to the moment of ignition of the EP discharge. In this experiment, directional stimulated detonation of an LEP is implemented. Note that the directed explosion of the LEP at the optimal value t_d was implemented and studied in our experiments for the first time. In this paper, we study the parameters of the shock waves (SWs) created by the directed explosion of an LEP.

3. SW CREATED BY THE MPC-EP. OPTIMAL DELAY TIME MODE t_d ~ 2000 μs

The general view of the laboratory setup is shown in Fig. 2. To study the parameters of SWs, pressure transducers (*2*), placed at specified distances from the combined MPC-EP discharger (*1*), were used. During the experiments, the pressure distribution $P_2(X)$ behind the front of the SW created by the MPC-EP and the average speed of the SW $V_{SW}(X)$ were measured.

A high-speed Photron FASTCAM Nova S9 (Photron, United States) video camera was used to study the structure, as well as the spatial and temporal evolution of the combined MPC-EP discharger (Fig. 3). During the experiments, it was discovered that in a certain range of delay times for switching on the MPC, the directed movement of the LEP occurs along the axis of the discharger, which can be characterized as the movement of a *plasma piston*, whose shape is close to cylindrical (see Fig. 3). Measurements carried out using pressure transducers revealed a strong anisotropy of the pressure distribution at the shock front near the boundary of the plasma piston, which is fundamentally different from the pressure distribution pattern measured in [2] for the case of the spherical stimulated detonation of an LEP. This result was also confirmed using the optical shadow method. At the optimal delay time for switching on the MPC of t_d ~ 2000 μs, the average velocity of the leading edge of the plasma jet (plasma piston) reaches V_{p2} ~ 1000–1200 m/s (hereinafter, index *p* means that the variable refers to the plasma piston). This value significantly exceeds the

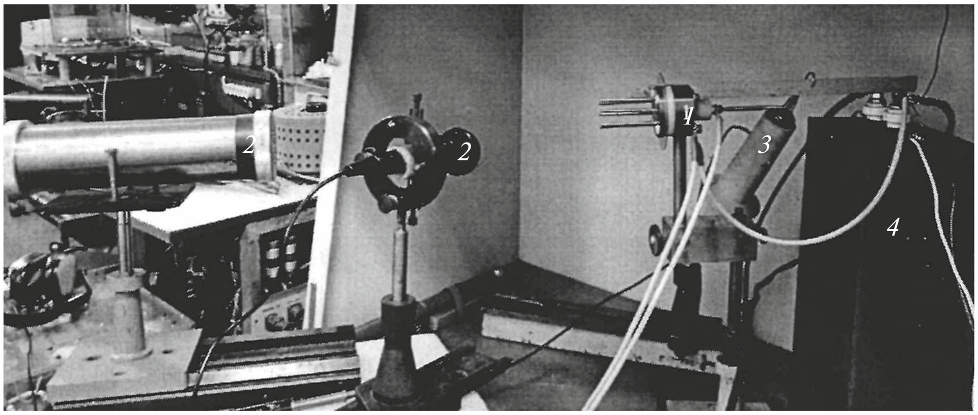

Fig. 2. General view of the laboratory setup: (*1*) MPC-EP combined discharger; (*2*) pressure transducers; (*3*) high-voltage probe P6015; (*4*) capacitive storage.

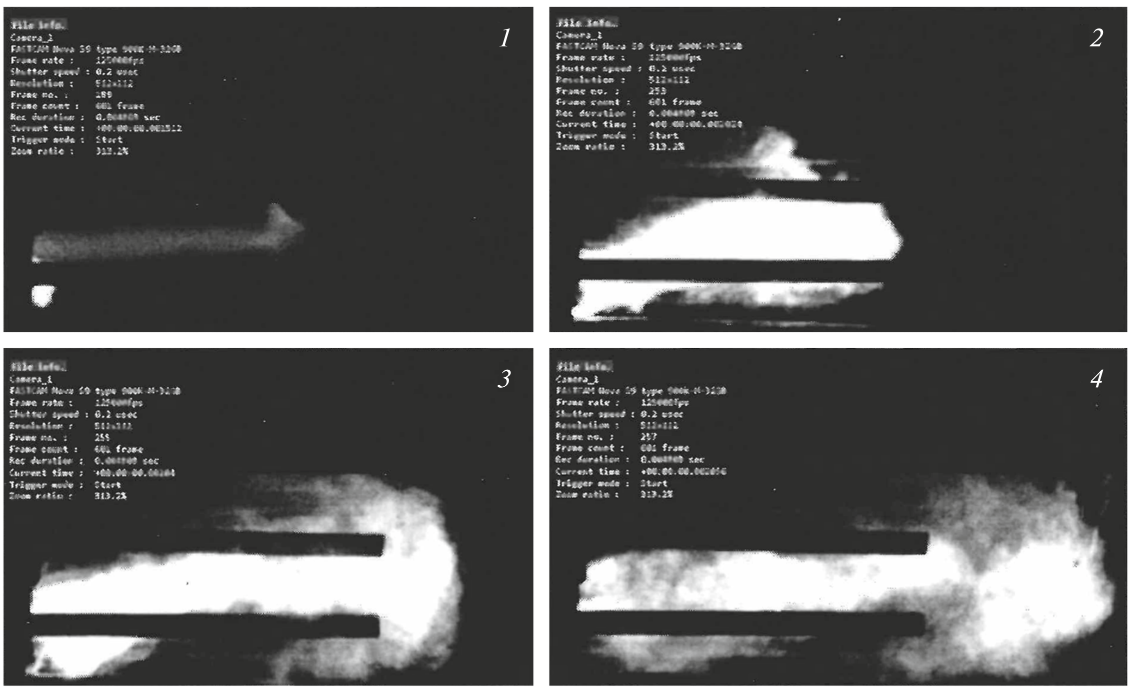

Fig. 3. High-speed video footage of the evolution of the plasma piston created by the MPC-EP: the delay time between turning on the EP and the MPC is t_d ~ 2000 μs, frame rate is 125000 fps, frame exposure time is 0.2 μs. Frame *1* corresponds to the state of the EP plasma jet before the MPC is turned on; frames (*2–4*) correspond to evolution of the plasma jet after turning on the MPC. Moments in time *t* relative to the beginning of the EP discharge: (*1*) 1512, (*2*) 2024, (*3*) 2040, (*4*) 2056 μs.

velocity of the leading edge of the plasma jet V_{p1} ~ 450–600 m/s, recorded in [2] at small delay times of t_d ~50 μs.

It has been established that when the EP uses only PMMA erosion products as a working fluid, the Mach number determined at a distance of X_1 = 30 cm from the output plane of the MPC-EP, where the ends of the cathode rods are located (*7* in Fig. 1), does not exceed a value of M_{SW} ~1.46. Thus, at distances of $X >$ 30 cm, a rather weak SW is formed and propagated. This result was obtained both by measuring the amplitude of the SW using a calibrated piezo pressure transducer and by measuring the velocity of its propagation (based on the time of arrival of the SW at the measuring pressure transducer). The difference in determining the Mach numbers using the listed methods does not exceed 3%.

As mentioned above, the average speed of the plasma piston reaches values of V_{p2} ~ 1000–1200 m/s. Its value was estimated as a result of processing individual frames of high-speed video recording (Fig. 3). From the analysis carried out, the value of the maximum

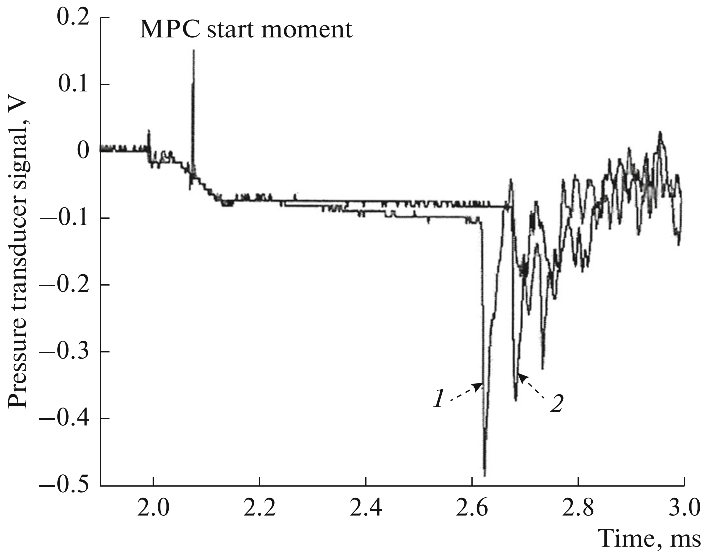

Fig. 4. Temporal evolution of pressure $P_2(t)$ behind the shock front, recorded by a pressure transducer: (*1*) working mixture of PMMA + TiH_x, (*2*) PMMA working mixture. Delay time between turning on the EP and the MPC is t_d ~ 2000 μs.

volume of the plasma piston, which was W_p ~ 130 cm^3, was also obtained.

To estimate the pressure P_2 behind the shock front with Mach number M_{SW} ~ 1.46 at a distance of X_1 = 30 cm, we use the known relation at the shock front:

$$P_2 = P_1\left(\frac{2\gamma}{\gamma+1}M^2 + \frac{\gamma-1}{\gamma+1}\right). \quad (1)$$

Here indices *1* and *2* correspond to the parameters in front of and behind the SW. From expression (1), we obtain that $P_2 = 2.5P_1$ (at $\gamma = 1.4$), and the pressure jump at the SW front is $\Delta P_2 = P_2 - P_1 = 1.5P_1 = 1.5$ bar.

In the weak SW approximation, it is possible to estimate the pressure jump at the shock front near the boundary of the plasma piston for X_2 ~ 10 cm (see Fig. 3):

$$\Delta P_2 \approx \left(\frac{30}{10}\right)^2 \times 1.5 = 13.5 \text{ bar}. \quad (2)$$

Then the detonation energy stored in the plasma piston can be defined as the product of the pressure jump (2) in the SW and the volume of the plasma piston W_p ~ 130 cm^3:

$$E_d = \Delta P_2 W_p = 175 \text{ J}. \quad (3)$$

Close values of the pressure jump ΔP_2^* and detonation energy E_d^* are obtained based on the measurement data of the plasma piston's velocity, V_p ~ 1100 m/s, (see above) using the well-known formula for SWs:

$$V_p = M_{SW}C_s(1 - \rho_1/\rho_2), \quad (4)$$

where C_s is the speed of sound, ρ_1 and ρ_2 are, respectively, the gas density in front of and behind the shock front.

From formula (4) we can obtain the desired Mach number M_{SW} ~ 3.8, and the pressure ratio reaches $(P_2/P_1)^*$ ~ 17 at the shock front when it is close to the boundary of the plasma piston. Then the pressure jump $\Delta P_2^* = P_2^* - P_1^*$ is of the order of magnitude ΔP_2^* ~ 16 bar, which is quite close to the value ΔP_2 = 13.5 bar, obtained by formula (2).

It was also found that the intensity of the SW largely depends on the composition of the working mixture. In the case when the composition of the working mixture is determined solely by the products of ablation of the capillary wall (PMMA), the pressure jump at the SW front is minimal. Adding TiH_x impurities to this mixture or NiH_x leads to the pressure behind the shock front increasing by approximately $P_2^{**}/P_2^* \approx 1.3$ times (Fig. 4). We assume that the additional pressure is related to the additional release of thermal energy δE_{ch} (index *ch* means a chemical source of energy release), initially stored in the internal degrees of freedom of the molecules of the activated working chemicals, due to the occurrence of specific plasma-chemical reactions in them [9–13]. Then this value can be estimated using the following relation:

$$\delta E_{ch} = 0.3E_d \approx 0.3 \times 175 = 52 \text{ J}.$$

According to the measurement results, the mass of the TiH_x impurity supplied to the volume of the plasma jet during the discharge pulse is δM_{er} = 1.2 mg/pulse. Therefore, the value of the specific additional energy can be estimated using the following formula:

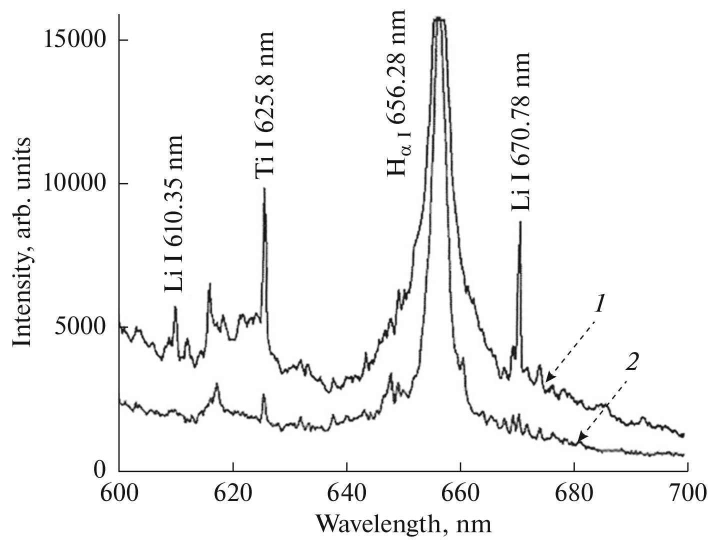

Fig. 5. Optical emission spectra of LEP: (*1*) emission spectrum upon injection of NiH_x impurity, (*2*) initial emission spectrum in the absence of impurity injection.

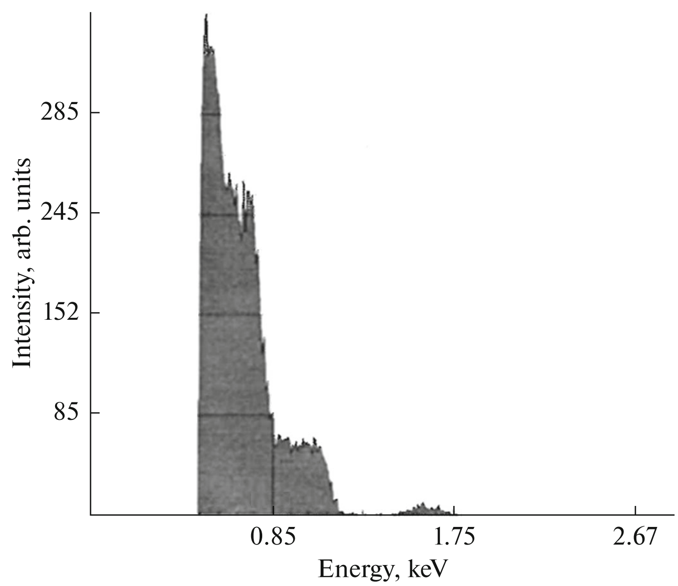

Fig. 6. Typical emission spectrum of an LEP in the X-ray range.

$$q_x = \frac{\delta E_{ch}}{\delta M_{er}} = \frac{52\ \text{J}}{1.2\ \text{mg}} = 43\ \text{kJ/g}.$$

Note that the value q_x exceeds the specific energy intensity of the trinitrotoluene (TNT) equivalent by a factor of 10:

$$K = \frac{q_x}{q_{\text{TNT}}} = \frac{43\ \text{kJ/g}}{4.2\ \text{kJ/g}} \approx 10.$$

Thus, the estimates show that the energy content of the LEP can reach large values.

4. OPTICAL AND X-RAY SPECTRA OF LEPs

The optical spectra of the LEP were recorded with an AvaSpec-ULS 2048 fiberoptic spectrometer (Avantes BV, Netherlands). In the emission spectra presented in Fig. 5, lines of excited atoms H, K, Ni, Na, Li, as well as fairly intense continuous emission, are observed. The presence of the latter is due to the formation of metal and carbon nanoclusters inside the LEP [2, 14]. Estimating the temperature of metal nanoclusters from continuous radiation in the Wien approximation leads to the following values: T ~3000–4000 K.

It was found that the additional injection of TiH_x particles into the discharge region of the MPC-EP leads to the appearance of intense Li I lines in the optical spectra: 610.35 and 670.78 nm (curve *1* in Fig. 5). Note the absence of these lines in the initial spectrum of the LEP emission, recorded without the injection of such an impurity (curve *2* in Fig. 5). This result is not entirely clear and requires detailed study in future experiments.

The X-123 spectrometer detected intense soft X-ray radiation with a quantum energy of the order of $E_x \sim 1$ keV (Fig. 6). In the same experiment, using the MKS-A03-1 radiometer-spectrometer (NPC "ASPEKT", Dubna), signals were recorded that can be interpreted as a flux of cold neutrons from the spatial region occupied by the LEP (see also [2, 14]). This result also requires further analysis and experimental verification.

5. CONCLUSIONS

1. For the first time, a combined discharger based on an MPC and a pulsed EP, MPC-EP, was designed, manufactured, and tested. This MPC-EP was used to study the physical properties of a high-energy, long-lived heterogeneous plasma formation over wide pressure and temperature ranges.

2. The pressure $P_2(t)$ behind the front of the SW created by the MPC-EP and the average velocity of the SW $V_{SW}(t)$ resulting from the stimulated detonation of the LEP were determined. It was found that with the optimal time delay of $t_d \sim 2000–4000$ μs between the moments of ignition of the EP and MPC discharges, the directed explosion mode of the LEP can be implemented. The measurements revealed a strong anisotropy of the pressure distribution behind the shock front. It was confirmed by the optical shadow method that in this mode a curved SW front, close to cylindrical, was formed.

3. It was found that in the range of the optimal MPC response delay times, the average front velocity of the plasma piston was $V_{p2} \sim 1000–1200$ m/s, which significantly exceeds the values of $V_{p1} \sim 450–500$ m/s recorded in the mode of small time delays ($t_d \sim 50$ μs) [2].

4. The dependence of the pressure jump at the shock front on the composition of the tested eroding materials (such as $C_5H_8O_2$, TiH_x, and NiH_x) filling the discharge gap of the MPC-EP, with all the other parameters of the electrical discharge being equal, was identified. Assuming that the additional energy release behind the SW front is related to the high-threshold plasma-chemical reactions with the participation of electrons of the inner electron shells occurring inside the LEP, it is possible to determine the value of the specific energy release of the reaction of $q_x \sim 43$ kJ/g. This assumption is confirmed by the LEP emission spectra recorded in the optical and X-ray wavelength ranges. Note that this specific additional energy released as a result of detonation q_x exceeds the specific energy of TNT by more than 10 times: $K = q_x/q_{TNT} \approx 10$. In this case, the value of K significantly exceeds the value measured in [2] at small delay times ($K^* = 2–4$ at $t_d \sim 50$ μs).

5. The authors assume that the experimental results obtained in this study will contribute to the development of ideas about the nature of electrophysical phenomena in a thunderstorm atmosphere, lower ionosphere, tornadoes, volcanic activity, and the appearance of natural plasmoids associated with them (such as ball lightning, sprites, jets, etc.) [15].

ACKNOWLEDGMENTS

The authors thank N.M. Ryazansky for his assistance in conducting the experimental studies.

FUNDING

This study was carried out with the support of the Russian Ministry of Science and Higher Education (state assignment no. 075-01129-23-00). No additional grants were received to conduct or direct this specific study.

CONFLICT OF INTEREST

The authors of this work declare that they have no conflicts of interest.

REFERENCES

1. I. C. Mashek, V. A. Lashkov, Y. F. Kolesnichenko, and V. G. Brovkin, in *49th AIAA Aerospace Sciences Meeting Including the New Horizons Forum and Aerospace Exposition* (Orlando, FL, 2011), AIAA paper 2011-1274. https://doi.org/10.2514/6.2011-1274
2. A. I. Klimov, N. K. Belov, V. G. Brovkin, and A. S. Pashchina, J. Phys. Conf. Ser. **2100**, 012006 (2021). https://doi.org/10.1088/1742-6596/2100/1/012006
3. A. K. Vinogradova and A. I. Morozov, "Stationary compression flows," in *Physics and Application of the Plasma Accelerators*, Ed. by A. I. Morozov (Nauka i Tekhnika, Minsk, 1974), pp. 103–141 [in Russian].
4. R. K. Rout, P. Mishra, A. M. Rawool, L. V. Kulkarni, and S. C. Gupta, J. Phys. D. Appl. Phys. **41** (20), 205211 (2008). https://doi.org/10.1088/0022-3727/41/20/205211
5. U. Shumlak, J. Appl. Phys. **127** (20), 200901 (2020). https://doi.org/10.1063/5.0004228
6. L. Soto, C. Pavéz, J. Moreno, L. Altamirano, L. Huerta, M. Barbaglia, A. Clausse, and R. E. Mayer., Phys. Plasmas **24** (8), 082703 (2017). https://doi.org/10.1063/1.4989845
7. R. Verma, R. S. Rawat, P. Lee, M. Krishnan, S. V. Springham, and T. L. Tan, Plasma Phys. Control. Fusion **51** (7), 075008 (2009). https://doi.org/10.1088/0741-3335/51/7/075008

8. A. S. Pashchina, A. V. Efimov, and V. F. Chinnov, High Temp. **55** (5), 650 (2017). https://doi.org/10.1134/S0018151X17040174
9. A. S. Pashchina and A. I. Klimov, Khim. Fiz. **33** (2), 78 (2014). https://doi.org/10.7868/S0207401X14020083
10. R. F. Avramenko, B. I. Bahtin, V. I. Nikolaeva, L. P. Poskacheeva, and N. N. Shirokov, Sov. Tech. Phys. **35** (12), 1396 (1990).
11. A. I. Klimov, Khim. Fiz. **25** (3), 104 (2006).
12. S. E. Emelin and A. L. Pirozersky, Khim. Fiz. **25** (3), 7 (2006).
13. *Ball Lightning in Laboratory (Collection of Papers)* (Khimiya, Moscow, 1994) [in Russian].
14. A. I. Klimov, N. K. Belov, and B. N. Tolkunov, J. Phys. Conf. Ser. **1698**, 012034 (2020). https://doi.org/10.1088/1742-6596/1698/1/012034
15. D. V. Nalivkin, *Hurricanes, Storms and Tornadoes* (Nauka, Leningrad, 1969) [in Russian].

Publisher's Note. Pleiades Publishing remains neutral with regard to jurisdictional claims in published maps and institutional affiliations.
AI tools may have been used in the translation or editing of this article.